DALTON

Molecular linear and quadratic non-linear optical properties of pentaammineruthenium complexes of coumarin dyes‡

Benjamin J. Coe,*,†,[a] Gareth Chadwick,[a] Stephan Houbrechts[b] and André Persoons[b,c]

[a] *Department of Chemistry, University of Manchester, Oxford Road, Manchester M13 9PL, UK*
[b] *Laboratory of Chemical and Biological Dynamics, Center for Research on Molecular Electronics and Photonics, University of Leuven, Celestijnenlaan 200D, B-3001 Leuven, Belgium*
[c] *Optical Sciences Center, University of Arizona, Tucson, AZ 85721, USA*

The ruthenium(II) complex salts $[Ru(NH_3)_5L][PF_6]_2$ [L = coumarin 510 (C-510) **1** or coumarin 523 (C-523) **2**] have been synthesized and fully characterized. Their Ru^{III} analogues $[Ru(NH_3)_5L][PF_6]_3$ (L = C-510 **3** or C-523 **4**) have been prepared by oxidation of **1** or **2**, respectively, with AgO_2CCF_3. Electronic spectroscopy and cyclic voltammetry have shown that the ruthenium centres exert an electron-withdrawing influence on the dyes, which is greater for C-523. The intense, low-energy intramolecular charge-transfer (i.c.t.) absorptions of the C-523 complexes displayed marked solvatochromism, whilst those of the C-510 complexes showed only very slight solvent dependence. Measurements of the first hyper-polarizability, β, by using the hyper-Rayleigh scattering technique at 1064 nm yielded large values in the range $(120–420) \times 10^{-30}$ esu, the largest being for $[Ru(NH_3)_5(C\text{-}523)][PF_6]_2$ **2**. These were enhanced by resonance *via* the i.c.t. excitations. Correction for resonance effects by using the two-level model afforded static hyper-polarizabilities (β_0) in the range $35–49 \times 10^{-30}$ esu, with $[Ru(NH_3)_5(C\text{-}523)][PF_6]_3$ **4** having the largest. The β_0 value for **4** was larger than that determined for C-523 *via* electric-field-induced second harmonic generation, indicating that complexation of a $\{Ru(NH_3)_5\}^{3+}$ moiety enhanced the hyper-polarizability of this dye. This has been ascribed to the electron-withdrawing effect of the Ru^{III} centre.

Over recent years there has been increasing interest in the study of organotransition-metal complexes for potential applications in non-linear optics (NLO).[1] Metal complexes are attractive in this context because they allow for combination of NLO with redox and/or magnetic properties, the metal centre functioning as an electron donor/acceptor group, or as part of a polarizable bridge. Much scope exists within this field for developments based upon novel synthetic co-ordination chemistry.

Complexes of ruthenium are ideal for the study of NLO effects because they combine appropriate redox and spectroscopic properties with an extensive co-ordination chemistry.[2] The most effective and useful method for the assessment of molecular NLO properties is by the solution measurement of hyper-polarizability coefficients (β for quadratic effects), which may be correlated directly with molecular structure. This eliminates the complications due to solid-state packing factors encountered when working with crystalline samples.[1] Several recent notable reports show that mixed-valence,[3] 2,2′-bipyridine (bipy),[4] and σ-acetylide[5] complexes of ruthenium can exhibit extremely large β values, although two-photon excited luminescence, rather than harmonic scattering, may explain these results for the bipy complexes.[6]

Coumarin dyes have promise for three major applications of chromophore-doped polymer NLO materials, *i.e.* in electro-optic,[7] frequency doubling[8] or photorefractive devices.[9] The first hyper-polarizabilities of a series of these dyes have recently been measured *via* electric-field-induced second harmonic generation (EFISHG), showing that coumarins 510 and 523 (Fig. 1) have the largest β values.[10] Since these compounds possess pyridyl and cyano groups, respectively, they are potential ligands for metals such as ruthenium. We hence sought to prepare diamagnetic complexes of these molecules with $\{Ru^{II}(NH_3)_5\}^{2+}$ centres, together with their paramagnetic ruthenium(III) analogues, and to measure their quadratic NLO properties by using the recently developed hyper-Rayleigh scattering (HRS) technique.[11,12] The HRS method has the important advantage over EFISHG in being applicable to charged compounds, such as complex salts. This study provides an opportunity to assess the effects of complexation and of metal-based redox changes on the NLO properties of these important organic molecules.

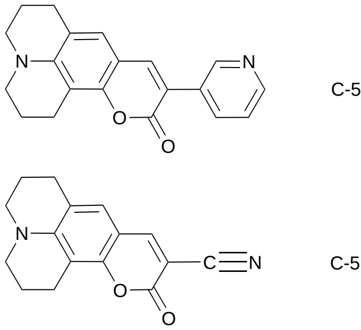

Fig. 1 Structures of coumarin 510 (C-510) and coumarin 523 (C-523)

Experimental

Materials and procedures

The laser dyes coumarin 510 and coumarin 523 (C-510 and C-523 respectively) were obtained from Exciton, $RuCl_3{\cdot}2H_2O$ was supplied by Johnson Matthey plc. The salts $[Ru^{III}Cl(NH_3)_5]Cl_2$ and $[Ru^{II}(NH_3)_5(H_2O)][PF_6]_2$ were prepared according to published procedures.[13,14] All other reagents were obtained commercially and used as supplied. All reactions were conducted in the dark. Products were dried overnight at room temperature in a vacuum desiccator ($CaSO_4$) prior to characterization.

Physical measurements

Proton NMR spectra were recorded on a Varian Gemini 200 spectrometer and all shifts are referenced to $SiMe_4$, elemental

---

† E-Mail: b.coe@man.ac.uk
‡ *Non-SI unit employed*: esu = 2.693×10^{20} C^3 m^3 J^{-2}.

analyses were performed by the Microanalytical Laboratory, University of Manchester. Infrared spectra were obtained as KBr discs with an ATI Mattson Genesis Series FTIR instrument, UV/VIS spectra were recorded using a Hewlett Packard 8452A diode array or a Varian Cary 1 spectrophotometer. Fast atom bombardment (FAB) mass spectra were recorded using a Kratos Concept spectrometer with a 6–8 keV (eV ≈ 1.60×10^{-19} J) Xe atom beam and 3-nitrobenzyl alcohol as matrix. Cyclic voltammetric measurements were carried out using an EG&G PAR model 173 potentiostat/galvanostat with a model 175 universal programmer. A single compartment cell was used with a saturated calomel electrode (SCE) as reference separated by a salt bridge from the platinum-bead working electrode and platinum-wire auxiliary electrode. Acetonitrile (HPLC grade) was used as received and tetra-*n*-butylammonium hexafluorophosphate, twice recrystallized from ethanol and dried *in vacuo*, was used as supporting electrolyte. Solutions containing *ca.* 10^{-3} mol dm^{-3} analyte (0.1 mol dm^{-3} electrolyte) were deaerated by purging with nitrogen. All $E_{\frac{1}{2}}$ values were calculated from $(E_{pa} + E_{pc})/2$ at a scan rate of 200 mV s^{-1}.

Syntheses

$[Ru^{II}(NH_3)_5(C\text{-}510)][PF_6]_2$ 1. To a stirring solution of coumarin 510 (C-510, 238 mg, 0.748 mmol) in Ar-degassed acetone (30 cm^3) was added $[Ru^{II}(NH_3)_5(H_2O)][PF_6]_2$ (250 mg, 0.506 mmol). The fluorescent yellow-green solution turned golden immediately and was stirred at room temperature under Ar for 3 h. The solution was reduced to a small volume *in vacuo*, and addition of diethyl ether gave a golden precipitate which was filtered off and washed with diethyl ether. The product was purified by several reprecipitations from diethyl ether–acetone to afford a golden solid, yield 250 mg (62%). $\delta_H(CD_3COCD_3)$ 9.03 (1 H, s, C_6H_4N), 8.71 (1 H, d, *J* 5.9 Hz, C_6H_4N), 8.03 (2 H, m, C_6H_4N and C_6H), 7.40–7.33 (1 H, m, C_6H_4N), 7.07 (1 H, s, CH), 3.37 (4 H, t, $2CH_2$), 3.11 (3 H, s, *trans*-NH_3), 2.86–2.75 (4 H, m, $2CH_2$), 2.65 (12 H, s, 4 × *cis*-NH_3), 2.03–1.93 (4 H, m, $2CH_2$). ν(C=O) 1676s cm^{-1} (Found: C, 30.35; H, 4.30; N, 12.10. Calc. for $C_{20}H_{33}F_{12}N_7O_2P_2Ru$: C, 30.25; H, 4.20; N, 12.35%). FAB mass spectrum: *m/z* 507 ($[M - 2PF_6^-]^+$) and 436 ($[M - 2PF_6^- - 4NH_3]^+$).

$[Ru^{II}(NH_3)_5(C\text{-}523)][PF_6]_2$ 2. This was synthesized and purified in an identical fashion to **1** by using coumarin 523 (C-523, 202 mg, 0.756 mmol) in place of C-510, and acetone (90 cm^3). The product was obtained as a dark red solid, yield 249 mg (66%). $\delta_H(CD_3COCD_3)$ 8.19 (1 H, s, C_6H), 7.03 (1 H, s, CH), 3.44 (4 H, t, $2CH_2$), 3.25 (3 H, s, *trans*-NH_3), 2.83–2.74 (4 H, m, $2CH_2$), 2.60 (12 H, s, 4 × *cis*-NH_3), 2.02–1.91 (4 H, m, $2CH_2$). ν(C≡N) 2186m cm^{-1}, ν(C=O) 1699s cm^{-1} (Found: C, 26.15; H, 3.80; N, 12.60. Calc. for $C_{16}H_{29}F_{12}N_7O_2P_2Ru$: C, 25.9; H, 3.95; N, 13.20%). FAB mass spectrum: *m/z* 598 ($[M - PF_6^-]^+$), 454 ($[M - 2PF_6^-]^+$), 437 ($[M - 2PF_6^- - NH_3]^+$), 420 ($[M - 2PF_6^- - 2NH_3]^+$), 401 ($[M - 2PF_6^- - 3NH_3]^+$) and 384 ($[M - 2PF_6^- - 4NH_3]^+$).

$[Ru^{III}(NH_3)_5(C\text{-}510)][PF_6]_3$ 3. To a solution of **1** (123 mg, 0.155 mmol) in acetone (10 cm^3) was added AgO_2CCF_3 (51.5 mg, 0.233 mmol). The reaction was stirred at room temperature for 20 min to give a green-yellow solution with a grey precipitate of silver metal. The mixture was filtered through Celite and the golden solution was reduced to a small volume *in vacuo*. Addition of aqueous NH_4PF_6 solution gave a golden precipitate which was filtered off, washed with water and dried, yield 116 mg (80%). ν(C=O) 1698s cm^{-1} (Found: C, 25.55; H, 3.55; N, 10.20. Calc. for $C_{20}H_{33}F_{18}N_7O_2P_3Ru$: C, 25.55; H, 3.55; N, 10.45%). FAB mass spectrum: *m/z* 506 ($[M - 2PF_6^-]^+$) and 436 ($[M - 2PF_6^- - 4NH_3]^+$).

$[Ru^{III}(NH_3)_5(C\text{-}523)][PF_6]_3$ 4. This was prepared and purified in identical fashion to **3** by using **2** (102 mg, 0.137 mmol) instead of **1**, acetone (6 cm^3) and AgO_2CCF_3 (45 mg, 0.204 mmol). The resulting orange-brown solution afforded the product as a red-brown solid, yield 110 mg (90%). ν(C≡N) 2242m cm^{-1}, ν(C=O) 1712s cm^{-1} (Found: C, 21.85; H, 3.30; N, 10.45. Calc. for $C_{16}H_{29}F_{18}N_7O_2P_3Ru$: C, 21.65; H, 3.30; N, 11.05%). FAB mass spectrum: *m/z* 598 ($[M - PF_6^-]^+$), 454 ($[M - 2PF_6^-]^+$), 437 ($[M - 2PF_6^- - NH_3]^+$), 420 ($[M - 2PF_6^- - 2NH_3]^+$), 401 ($[M - 2PF_6^- - 3NH_3]^+$) and 384 ($[M - 2PF_6^- - 4NH_3]^+$).

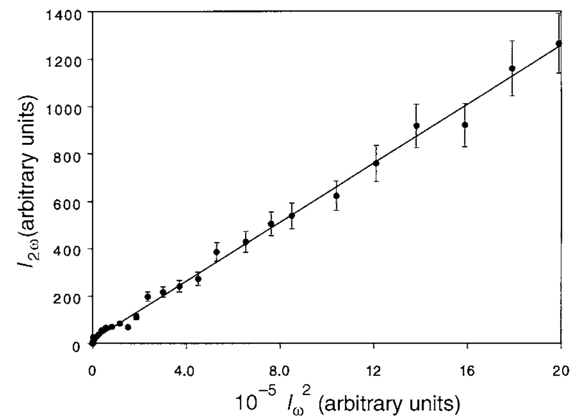

Fig. 2 Second harmonic generated intensity *vs.* the squared fundamental intensity in an HRS experiment; experimental data and linear fit for salt **2** in acetonitrile (4.68×10^{-6} mol dm^{-3}). Error bars are at 10% of the *y* value

Hyper-Rayleigh scattering

The experimental set-up used was as described in a recent report.[15] Infrared laser pulses generated with an injection seeded, Q-switched Nd-YAG laser (Quanta-Ray GCR-5, 1064 nm, 8 ns pulses, 7 mJ, 10 Hz) were focused into a cylindrical cell (7 cm^3). Rotation of a half-wave plate placed between crossed polarizers modulates the fundamental intensity which was measured with a photodiode. The light scattered at the second harmonic (532 nm) was collected by an efficient condenser system and detected with a photomultiplier. Discrimination of the harmonic from the fundamental light was accomplished by a low-pass filter and a 532 nm interference filter. Actual values for the intensities were retrieved using gated integrators. In all experiments the incident light was vertically polarized along the *z* axis.

All measurements were performed in acetonitrile and the known hyper-polarizability of *p*-nitroaniline in this solvent (29.2×10^{-30} esu)[16] was used as an external reference. The more recent external reference method has been found to give more reliable β values than the originally used internal reference method.[17–20] All samples were passed through a 0.45 mm filter (Millipore) to avoid spurious signals due to particulate scattering, and were checked for fluorescence which can interfere with the HRS signal.[6,21,22]

The theory of HRS has been dealt with previously.[11,12,15,23] However, we include here a brief description of the method used to extract the molecular first hyper-polarizability from the experimental data. The intensity of the scattered harmonic light is quadratically dependent upon the fundamental intensity (Fig. 2). For a solvent–solute system, this relation can be expressed in equation (1) where N_S and N_s are the concentrations of the solvent and solute, respectively, and *g* is an instrumental factor which takes into account the scattering geometry, photomultiplier gain and collection efficiency.

$$\frac{I_{2\omega}}{I_\omega^2} = g(N_S\beta_S^2 + N_s\beta_s^2) \qquad (1)$$

In a HRS experiment the ratio $I_{2\omega}/I_\omega^2$ is determined for a

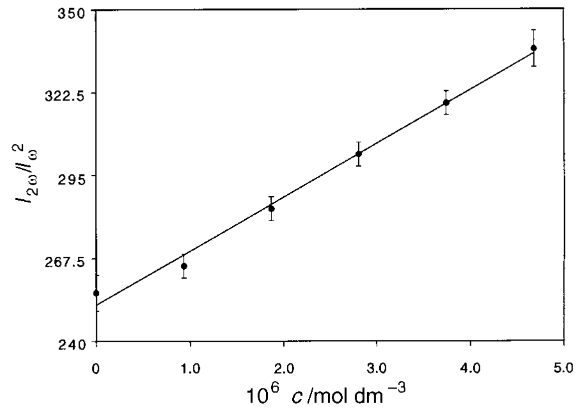

Fig. 3 Ratio of the intensities $I_{2\omega}/I_{2\omega}{}^2$ *vs.* the molar concentration; experimental data and linear fit for salt **2** in acetonitrile. Each point is the average of four separate measurements and error bars show the standard deviations

dilution series of the solute. For molecules non-absorbing at the second harmonic frequency, this ratio depends linearly upon the solute concentration. If absorption occurs at the harmonic frequency, as is the case for the salts **1**–**4** (Table 3), a Lambert–Beer correction factor must be included in equation (1). However, if low concentrations (10^{-4}–10^{-5} mol dm^{-3}) are used, such that concentration × pathlength × absorption coefficient < 0.05, then this correction factor becomes negligible and a linear dependence is observed (Fig. 3). This approach minimizes the errors on the slopes, and thus on the hyper-polarizabilities which are calculated from the ratio of the slopes of the sample and reference [equation (2)].

$$\frac{g\beta^2_{\mathbf{sample}}}{g\beta^2_{\mathbf{ref}}} = \frac{\text{sample slope}}{\text{reference slope}} \qquad (2)$$

The HRS method determines the averaged hyper-polarizability in laboratory coordinates $\langle\beta^2\rangle$ which is related to the hyper-polarizability in the molecular reference system by a complex summation of weighted products of tensor components.[23,24] For a molecule with C_{2v} symmetry (*e.g.* *p*-nitroaniline) the relation can be expressed as in equation (3) where

$$\langle\beta^2\rangle = \langle\beta_{zzz}{}^2\rangle + \langle\beta_{xzz}{}^2\rangle \qquad (3)$$

$\langle\beta_{zzz}{}^2\rangle$ and $\langle\beta_{xzz}{}^2\rangle$ are defined in equations (4) and (5) respectively.

$$\langle\beta_{zzz}{}^2\rangle = \frac{1}{7}\,\beta_{333}{}^2 + \frac{6}{35}\,\beta_{333}\beta_{322} + \frac{9}{35}\,\beta_{322}{}^2 \qquad (4)$$

$$\langle\beta_{xzz}{}^2\rangle = \frac{1}{35}\,\beta_{333}{}^2 - \frac{2}{105}\,\beta_{333}\beta_{322} + \frac{11}{105}\,\beta_{322}{}^2 \qquad (5)$$

The letter indices refer to the laboratory frame and the number indices to the molecular frame. For simplicity, we have assumed here that the tensor components in the plane of the molecule are dominant. For the complexes under investigation, we assume these tensor components to be in the plane of the coumarin segment with the major component directed along the intramolecular charge-transfer axis and a smaller component perpendicular to this axis. In this sense, the complexes are treated as resembling C_{2v} molecules such as *p*-nitroaniline. Due to the low concentrations used, harmonic intensities were insufficient to allow depolarization measurements.

Results and Discussion

Synthetic studies

The new complex salts $[\text{Ru}^{\text{II}}(\text{NH}_3)_5\text{L}][\text{PF}_6]_2$ (L = C-510 **1** or C-523 **2**) were prepared in a straightforward fashion by reaction of $[\text{Ru}^{\text{II}}(\text{NH}_3)_5(\text{H}_2\text{O})][\text{PF}_6]_2$ with the appropriate ligand. The identity and purity of the products was confirmed by elemental analyses and ^{1}H NMR spectroscopy. Salt **1**, being more sensitive to oxidation (see later), is the more difficult complex to obtain in pure form, and contamination by its ruthenium(III) analogue is easily detected by paramagnetic broadening in the ^{1}H NMR spectrum. Ruthenium oxidation by AgO_2CCF_3 occurs readily, producing $[\text{Ru}^{\text{III}}(\text{NH}_3)_5\text{L}][\text{PF}_6]_3$ (L = C-510 **3** or C-523 **4**) in high yield. The presence of the intact coumarin ligands in salts **3** and **4** is confirmed by elemental analyses, infrared spectroscopy and FAB mass spectrometry. The structures of the complexes are shown in Fig. 4.

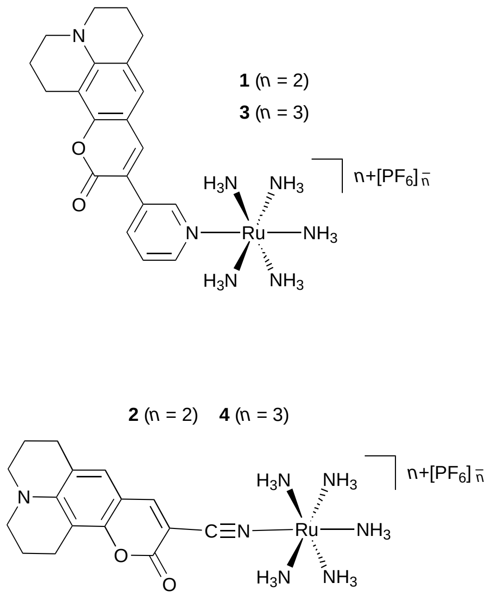

Fig. 4 Structures of the cations in the salts **1**–**4**

Infrared spectroscopy studies

The intense ν(C≡N) band of C-523 at 2205 cm^{-1} undergoes a low energy shift of 19 cm^{-1}, accompanied by a reduction in intensity, on co-ordination to give salt **2**. Similar effects have been observed previously in related complexes of benzonitrile,[25] acetonitrile[25] and 4-cyanopyridine,[26] and are attributed to the unusually strong π back-bonding ability of the $\{\text{Ru}^{\text{II}}(\text{NH}_3)_5\}^{2+}$ moiety. Oxidation to give **4** produces high energy shifts in the ν(C≡N) band of 56 cm^{-1} from **2** and of 37 cm^{-1} from C-523 owing to the electron-withdrawing effect of the $\{\text{Ru}^{\text{III}}(\text{NH}_3)_5\}^{3+}$ centre. This also parallels observations made in related organonitrile complexes.[25,26] The ν(C=O) bands which occur in the unco-ordinated coumarins at 1697 cm^{-1} (C-510) and at 1716 cm^{-1} (C-523) are shifted to low energy in the Ru$^{\text{II}}$ salts **1** and **2**, but are unshifted in the Ru$^{\text{III}}$ salts **3** and **4**. This can also be attributed to the π* electron-donating influence of the $\{\text{Ru}^{\text{II}}(\text{NH}_3)_5\}^{2+}$ moieties.

Proton NMR spectroscopy studies

Resonances for all of the ligand protons are observed in salts **1** and **2**, and the $\{\text{Ru}^{\text{II}}(\text{NH}_3)_5\}^{2+}$ units give two broad singlets in a 4:1 ratio for the *cis*- and *trans*-ammine ligands, respectively. The latter are deshielded with respect to the former due to the *trans*-coumarin ligands, to the extent of 0.46 ppm in **1** and 0.65 ppm in **2**. The *trans*-ammine signal in **2** is found to low field of that in **1** by 0.14 ppm, due to the lower basicity of the cyano group of C-523 compared with the pyridyl group of C-510.

Electronic spectroscopy studies

Electronic spectra for the new complex salts were recorded in

Table 1 Electrochemical and UV/VIS data for complex salts and coumarins in acetonitrile

Complex salt/coumarin	$E_{\frac{1}{2}}{}^{a}$/V *vs.* SCE (ΔE_p/mV) $\mathrm{Ru^{III/II}}$	Coumarin		$\lambda_{max}{}^{b}$/nm (ε/dm^3 mol^{-1} cm^{-1})	Assignment
1 $[\mathrm{Ru^{II}(NH_3)_5(C\text{-}510)}][\mathrm{PF_6}]_2$	0.37 (70)	0.85 (60)	-1.70^c	216 (27 100)^d	$\pi \longrightarrow \pi^*$
				252 (9200)	$\pi \longrightarrow \pi^*$
				274 (8300)	$\pi \longrightarrow \pi^*$
				430 (38 500)	i.c.t./m.l.c.t.
2 $[\mathrm{Ru^{II}(NH_3)_5(C\text{-}523)}][\mathrm{PF_6}]_2$	0.51 (65)	1.14 (70)	-1.48^c	220 (24 200)^d	$\pi \longrightarrow \pi^*$
				240sh (17 500)	$\pi \longrightarrow \pi^*$
				278sh (11 700)	$\pi \longrightarrow \pi^*$
				408 (13 000)	m.l.c.t.
				498 (38 900)	i.c.t.
3 $[\mathrm{Ru^{III}(NH_3)_5(C\text{-}510)}][\mathrm{PF_6}]_3$				218 (30 400)^d	$\pi \longrightarrow \pi^*$
				261 (11 000)	$\pi \longrightarrow \pi^*$
				438 (35 900)	i.c.t.
4 $[\mathrm{Ru^{III}(NH_3)_5(C\text{-}523)}][\mathrm{PF_6}]_3$				224 (28 900)^d	$\pi \longrightarrow \pi^*$
				268 (14 500)	$\pi \longrightarrow \pi^*$
				460 (40 900)	i.c.t.
				500sh (23 400)	i.c.t.
C-510		0.76 (60)	-1.83^c	218 (28 800)^d	$\pi \longrightarrow \pi^*$
		1.76^e		272 (9400)	$\pi \longrightarrow \pi^*$
				418 (34 100)	i.c.t.
C-523		0.99 (70)	-1.48^c	218 (35 300)^d	$\pi \longrightarrow \pi^*$
		2.13^e		266 (12 500)	$\pi \longrightarrow \pi^*$
				444 (54 900)	i.c.t.

[a] Measured in solutions *ca.* 10^{-3} mol dm^{-3} in analyte and 0.1 mol dm^{-3} in $\mathrm{NBu^n{}_4PF_6}$ at a Pt-bead working electrode with a scan rate of 200 mV s^{-1}, ferrocene internal reference $E_{\frac{1}{2}} = 0.41$ V, $\Delta E_p = 60$ mV. [b] Solutions (1–4) × 10^{-5} mol dm^{-3}. [c] E_{pc} for an irreversible reduction process. [d] Maximum of a band showing vibrational fine structure. [e] E_{pa} for an irreversible oxidation process.

acetonitrile and results are presented, together with data for the coumarin ligands, in Table 1. The free dyes exhibit intense, broad absorptions to high energy in the visible region due to intramolecular charge-transfer (i.c.t.) excitations, corresponding to electron transfer from the tertiary amino donor to the vinyl lactone acceptor groups.[27] It is emission from these i.c.t. states which gives rise to the characteristic fluorescence of the coumarins and their resulting application as laser dyes.[28,29]

Complexation of C-510 to produce **1** causes a small red shift of 12 nm in the i.c.t. band, but otherwise has very little effect on the spectrum. The spectrum of **3** is also very similar to that of the free dye, with a red shift of 20 nm in the i.c.t. band. The $d_\pi(\mathrm{Ru^{II}}) \longrightarrow \pi^*$ (pyridyl) metal-to-ligand charge-transfer (m.l.c.t.) absorption in **1**, expected to lie in the region 400–450 nm,[30] is clearly obscured by the more intense coumarin i.c.t. band.

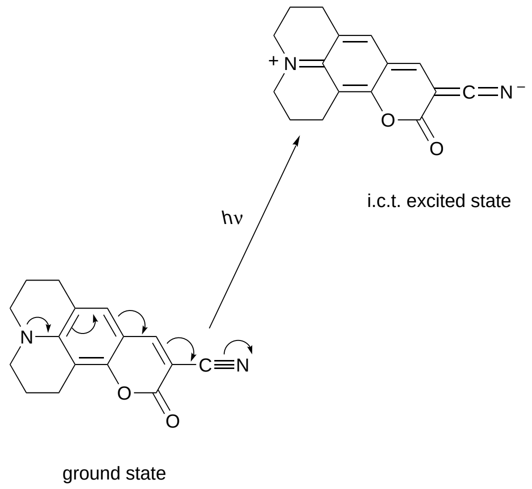

Fig. 5 Simplified representation of the formation of one possible i.c.t. excited state of C-523

Co-ordination of C-523 to produce **2** causes a marked change in the absorption profile, giving a deep red complex exhibiting two distinct visible bands. The less intense, high-energy band at 408 nm is assigned to a $d_\pi(\mathrm{Ru^{II}}) \longrightarrow \pi^*$ (cyano) m.l.c.t. absorption,[25] at relatively low energy due to the electron-withdrawing effect of the vinyl lactone unit. The band at 498 nm, which is very intense but somewhat less so than that of the free C-523 at 444 nm, is ascribed to the dye i.c.t. absorption red shifted by 54 nm on co-ordination. This band is broadened considerably by complexation, with bandwidth (full width at half maximum, f.w.h.m.) values being 48 nm for C-523 and 84 nm for **2**. The red shift shows that the $\{\mathrm{Ru^{II}(NH_3)_5}\}^{2+}$ moiety exerts an electron-withdrawing influence on the π system of the coumarin ligand. This is in contrast with the electron-donating effect of the $\mathrm{Ru^{II}}$ centre on the ligand π* system shown by infrared (see earlier), and can be understood by a simplified consideration of the i.c.t. process. The resonance structure of one i.c.t. excited state of C-523 in which charge migrates to the cyano acceptor group is shown in Fig. 5. Attachment of the dicationic Ru centre to the cyano group will stabilize the negative charge and hence lower the energy of this i.c.t. transition. A similar charge delocalization to the site of co-ordination is precluded in the C-510 complexes by the 3-substitution on the pyridyl ring, explaining the much greater influence of the co-ordinated $\{\mathrm{Ru(NH_3)_5}\}^{n+}$ ($n = 2$ or 3) moiety on the i.c.t. band of C-523 compared with that of C-510.

The oxidized form of **2** (*i.e.* **4**) shows only a single discernible visible band at 460 nm with a shoulder at *ca.* 500 nm. In addition to the visible absorption bands, the complexes and ligands show intense, high energy bands below 300 nm due to $\pi \longrightarrow \pi^*$ excitations. The UV/VIS absorption spectra of C-523, **2** and **4** are shown in Fig. 6. None of the complex salts shows any luminescence upon excitation at 532 nm, precluding spurious contributions to HRS signals from two-photon excited luminescence.[6] However, **1** does luminesce under higher-energy excitation into the i.c.t. band at 430 nm.

It is well established that solvatochromism is often an indicator of substantial molecular β values.[31] The visible absorption spectra of the C-510 salts **1** and **3** show almost no solvent dependence, but the C-523 salts **2** and **4** exhibit marked effects. The results of a solvatochromism study with these two salts and with C-523 are presented in Table 2. The i.c.t. band for the free C-523 is almost independent of solvent, but for **2** marked

Table 2 Solvatochromism and solvent data for coumarin 523 and for salts **2** and **4**

		Donor number^{b}/	C-523	**2**			**4**		
Solvent	ε_r^{a}	kcal mol^{-1}	λ_{max}/nm	λ_{max}/nm ($E_{i.c.t.}$, $\times 10^{-3}$ cm^{-1})		m.l.c.t. : i.c.t.	λ_{max}/nm		
Hexamethylphosphoramide (hmpa)	31.3	38.8	442	410	562 (17.79)	1.22		456	
Dimethyl sulfoxide	47.2	29.8	448	418	544 (18.38)	0.77	424	454	536
Dimethylformamide (dmf)	38.3	26.6	446	414	530 (18.87)	0.67	420	450	524
Trimethyl phosphate	20.6	23.0	442	412	520 (19.23)	0.65		458	498 (sh)
Pyridine	13.3	33.1	448	416	516 (19.38)	0.45		450	492 (sh)
Methanol	33.0	19	444	412	508 (19.69)	0.39		458	504 (sh)
Acetone	21.0	17.0	442	410	506 (19.76)	0.40		460	502 (sh)
Water	80.1	18.0	*c*	416	506 (19.76)	0.30		468	516 (sh)
Acetonitrile	36.6	14.1	444	408	498 (20.08)	0.33		460	500 (sh)
Nitromethane	37.3	2.7	448		496 (20.16)			458	510 (sh)
$\Delta\lambda$/nm^{d}			6	10	66			18	34
ΔE/cm^{-1}^{e}			303	586	2368			855	1668

[a] ε_r = relative permittivity (dielectric constant) of solvent at 20 °C.[32] [b] Gutmann donor number,[33] cal = 4.184 J. [c] Insoluble. [d] Difference between maximum and minimum λ_{max} values. [e] Difference between maximum and minimum energies.

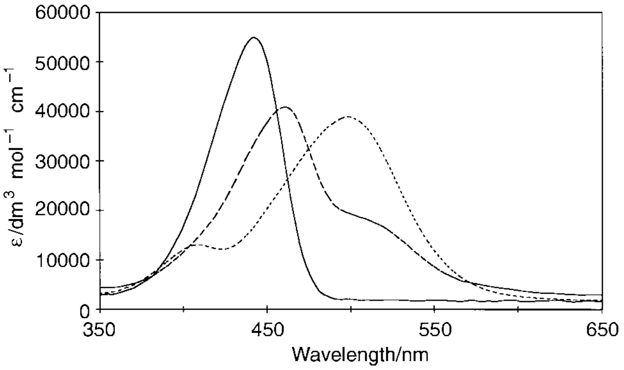

Fig. 6 The UV/VIS spectra of compounds C-523 (——), **2** (---) and **4** (– – –) in acetonitrile

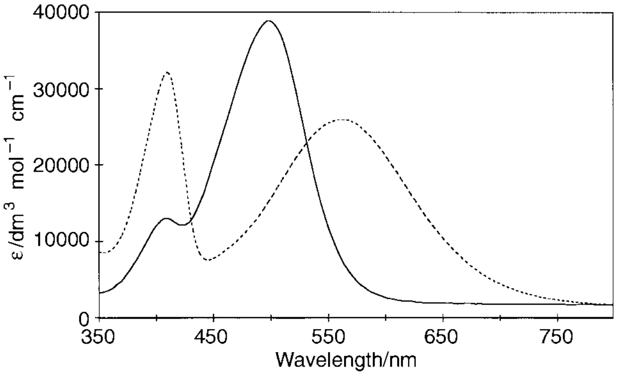

Fig. 7 The UV/VIS spectra of salt **2** in acetonitrile (——) and in hmpa (---)

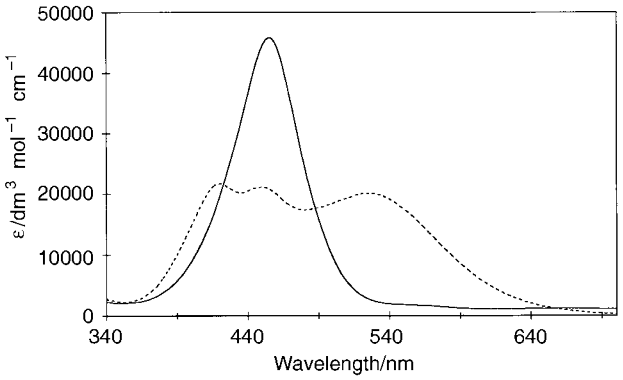

Fig. 8 The UV/VIS spectra of salt **4** in hmpa (——) and in dmf (---)

colour changes from orange (nitromethane) through red (acetone) to purple (hexamethylphosphoramide, hmpa) are observed. The position of the low energy coumarin i.c.t. band shifts much more than does that of the m.l.c.t. band, but the relative intensity of the latter increases dramatically as the i.c.t. band moves to lower energy. In acetonitrile the m.l.c.t. band is at 408 nm (ε = 13 000 dm^3 mol^{-1} cm^{-1}) and the i.c.t. band at 498 nm (ε = 38 900 dm^3 mol^{-1} cm^{-1}), whereas in hmpa the m.l.c.t. band is at 410 nm (ε = 32 200 dm^3 mol^{-1} cm^{-1}) and the i.c.t. band at 562 nm (ε = 26 000 dm^3 mol^{-1} cm^{-1}) (Fig. 7). In nitromethane the m.l.c.t. band is not observed, presumably being obscured by the solvent cut-off at *ca.* 400 nm. The i.c.t. bandwidth increases steadily with decreasing energy, giving a f.w.h.m. of 135 nm in hmpa.

The low-energy shoulder observed on the major absorption band of **4** in acetonitrile is almost resolved in water due to a red shift, but in hmpa the yellow solution exhibits only a single, symmetrical band at 456 nm (ε = 45 800 dm^3 mol^{-1} cm^{-1}) (Fig. 8). Salt **4** has a very different visible spectrum in dimethylformamide (dmf) or dimethyl sulfoxide which contains three resolved bands of comparable intensity. In dmf the pink solution has band maxima at 420 nm (ε = 21 700 dm^3 mol^{-1} cm^{-1}), 450 nm (ε = 21 200 dm^3 mol^{-1} cm^{-1}) and 524 nm (ε = 20 100 dm^3 mol^{-1} cm^{-1}) (Fig. 8). Further investigations are required to explain this behaviour, and the possibility of solvolysis reactions cannot be eliminated at this stage.

Previous studies on the solvatochromism in dipolar aprotic solvents of ruthenium ammine complexes show that the m.l.c.t. band energies do not correlate with solvent relative permittivity, but rather with the solvent (Gutmann) donor numbers.[14] This was rationalized by invoking hydrogen bonding between solvent molecules and ammine ligands which increases the electron density at the Ru centre, stabilizing Ru^{III}, and hence shifting the m.l.c.t. transition to lower energy. Further support for this hypothesis was obtained by good correlations between m.l.c.t. absorption energies and other solvent scales which are based on the hydrogen-bond-accepting ability of the solvent.[14]

For **2**, there is no correlation between the m.l.c.t. energy and the Gutmann donor numbers,[33] but a plot of the i.c.t. energy ($E_{i.c.t.}$) against donor numbers does show a good correlation, with the notable exceptions of nitromethane and pyridine (Fig. 9). Pyridine was not included in the aforementioned study.[14] According to the hypothesis described above, hydrogen bonding will reduce the electron-withdrawing effect of the $\{Ru^{II}(NH_3)_5\}^{2+}$ centre, destabilizing the complexed i.c.t. excited state shown in Fig. 5. This would cause a blue shift in the i.c.t. absorption with increasing donor number. That an opposite trend is observed shows that the i.c.t. state is in fact stabilized by more strongly donating solvents. This can be ascribed to a

Table 3 Linear and non-linear optical data[a]

Complex salt/coumarin	λ_{max}/nm	ε_{532}[b]/dm^3 mol^{-1} cm^{-1}	10^{-30} β_{1064}[c]/esu	10^{-30} β_0[c]/esu
1 $[Ru^{II}(NH_3)_5(C\text{-}510)][PF_6]_2$	430	300	120	35
2 $[Ru^{II}(NH_3)_5(C\text{-}523)][PF_6]_2$	498	22 100	420	41
3 $[Ru^{III}(NH_3)_5(C\text{-}510)][PF_6]_3$	438	700	137	37
4 $[Ru^{III}(NH_3)_5(C\text{-}523)][PF_6]_3$	460	13 600	240	49
C-510	418	0	114	33
C-523	444	1 800	132	32

[a] Spectra for complex salts recorded in acetonitrile; NLO data for free coumarins recorded by EFISHG in chloroform.[10] [b] Extinction at the second harmonic wavelength of 532 nm. [c] The value of β_{1064} is the uncorrected first hyper-polarizability measured using a 1064 nm Nd-YAG laser fundamental (15% error); β_0 is the static hyper-polarizability estimated by using the two-level model [Equation (6)].

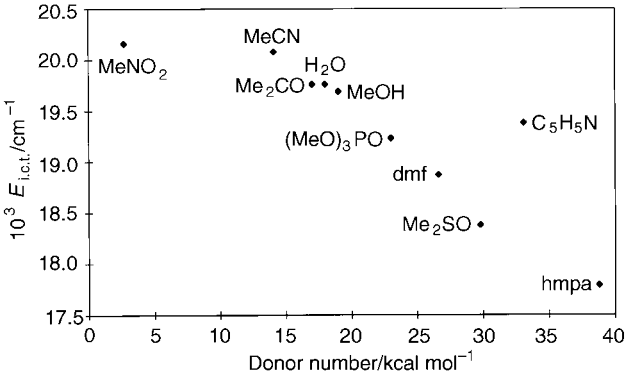

Fig. 9 A plot of the i.c.t. energy ($E_{i.c.t.}$) *vs.* the solvent Gutmann donor number for salt **2**

solvent-induced (inner-sphere) stabilization of the ammonium end of the excited state molecule which is more significant than the (outer-sphere) destabilization of the complexed acceptor portion.

Electrochemical studies

The ruthenium(II) complexes and coumarins were studied by cyclic voltammetry in acetonitrile and results are presented in Table 1. The free dyes exhibit three well-separated redox waves due to a reversible oxidation, an irreversible oxidation and an irreversible reduction process. The reversible wave is assigned to a one-electron oxidation of the tertiary amine donor group. All three waves occur to more positive potential in C-523 than in C-510 due to the greater electron-withdrawing effect of the cyano group compared with the 3-pyridyl group.

In addition to waves associated with the coumarin ligands, the complexes also show reversible $Ru^{III/II}$ oxidation waves at potentials which are less positive than those of the reversible ligand waves. As expected, **1** has the less positive $Ru^{III/II}$ $E_{\frac{1}{2}}$ value due to destabilization of the Ru-based highest occupied molecular orbital by the more basic pyridyl ligand (C-510). The reversible ligand-based oxidations are shifted upon complexation, by +90 mV for C-510 (in **1**) and by +150 mV for C-523 (in **2**). These shifts show that the $\{Ru^{III}(NH_3)_5\}^{3+}$ centre exerts an electron-withdrawing influence on the coumarin molecules which is more significant with C-523 than with C-510. This can be ascribed to the greater oxidizing strength of the cyano-bound Ru^{III} moiety, together with the improved metal–ligand electronic coupling *via* the cyano group, also observed in the UV/VIS spectra.

Non-linear optical studies

The second-order NLO susceptibilities of the new complexes were measured in acetonitrile using the HRS technique[11,12,15] with a 1064 nm Nd-YAG laser fundamental. Results are presented in Table 3, together with the visible band maxima and EFISHG data for the coumarin dyes in chloroform.[10]

Meaningful data for the coumarins could not be obtained using our HRS set-up because incoherent fluorescence is indistinguishable from the scattered second harmonic at 532 nm. It has recently been demonstrated that this problem may be overcome by conducting time-resolved HRS experiments.[34] It is established that compounds which display solvatochromism also show solvent-dependent first hyper-polarizabilities.[16] Since the coumarins used in this study show almost no solvatochromism [i.c.t. λ_{max} values are 446 nm ($CHCl_3$) and 444 nm (MeCN) for C-523, and 422 nm ($CHCl_3$) and 418 nm (MeCN) for C-510], it can be assumed that their β values in acetonitrile will be indistinguishable from those reported in chloroform.[10] Given that β values for standard dipolar NLO organics obtained *via* HRS generally agree closely with those derived from EFISHG,[11,12] the data reported here for the complexes are expected to be compatible with those reported for the dyes.[10]

The β values obtained for the new complexes are large, and comparable with those previously reported for various other Ru complexes.[3–5] These β values are resonantly enhanced due to strong absorption in the region of the second harmonic at 532 nm (Table 3). This phenomenon can be explained by means of the two-level model.[35] According to this approximation, the relationship between the first hyper-polarizability and the optical charge transfer (o.c.t.) excitation, which is the main contributor to β, is described by equation (6) where $h\omega_{o.c.t.}$ is the

$$\beta(-2\omega;\omega,\omega) = \frac{3\Delta\mu M^2}{(h\omega_{o.c.t.})^2}\,\frac{\omega_{o.c.t.}^{\ 2}}{[1-(2\omega)^2(\omega_{o.c.t.}^{\ 2})^{-1}][(\omega_{o.c.t.})^2-\omega^2]}$$
$$= \beta_0\,\frac{\omega_{o.c.t.}^{\ 2}}{[1-(2\omega)^2(\omega_{o.c.t.}^{\ 2})^{-1}][(\omega_{o.c.t.})^2-\omega^2]} \qquad (6)$$

energy of the o.c.t. excitation, Δμ is the change in dipole moment between the ground state and excited state, *M* is the electronic transition moment, ω is the fundamental laser frequency and β_0 is the static hyper-polarizability. Values of β_0 calculated using equation (1), with $h\omega_{o.c.t.}$ being the frequency (in cm^{-1}) of the i.c.t. absorption, are listed in Table 3. The assumption that the i.c.t. excitation is the principal contributor to β is supported by the marked solvatochromism of this band, at least in the case of **2** (see earlier). Since a neglect of damping in the two-level model causes underestimation of β_0 when the absorption maximum is close to the second harmonic frequency, the β_0 values for **2** and **4** are likely to be artificially low (**4** displays a shoulder at *ca.* 500 nm).

The complexes of C-523 have apparently larger β_0 values than do those of C-510, but the small differences are within experimental error. This is unsurprising because the two dyes also have experimentally indistinguishable corrected hyper-polarizabilities.[10] The ruthenium(III) complexes have slightly larger β_0 values than their ruthenium(II) analogues, the contrast being greater for the C-523 complexes, but again these differences may not be significant.

The similarity of the β and β_0 values for compounds **1**, **3** and C-510 shows that complexation has a negligible effect on the hyper-polarizability. This is in keeping with the slight differences in the linear optical properties found in the UV/VIS spectra. The value of β is markedly enhanced in **2** and **4** with respect to C-523 due to the red shifting of the i.c.t. absorption. These complexes also have larger estimated static hyper-polarizabilities than C-523, indicating that complexation enhances the first hyper-polarizability of this dye. The increase for **2** may not be experimentally significant, but that for **4** is larger. These observations are consistent with the infrared, electrochemical and UV/VIS data which show that the electronic influence of the $\{Ru(NH_3)_5\}^{n+}$ ($n = 2$ or 3) unit is most effectively communicated to the ligand *via* the cyano group, and that the Ru^{III} centre is the more electron-withdrawing.

Conclusion

Coumarin laser dyes form complexes of the type $[Ru(NH_3)_5L]^{n+}$ ($n = 2$ or 3; L = coumarin-510 or -523) which exhibit large first hyper-polarizabilities at 1064 nm due in part to resonance enhancement. Estimated static hyper-polarizabilities indicate that the NLO susceptibility of the dye is enhanced to a small extent in the C-523 complexes. This can be attributed to the electron-withdrawing influence of the $\{Ru(NH_3)_5\}^{n+}$ ($n = 2$ or 3) moiety attached to the acceptor portion of the molecule, which is greater when $n = 3$. Further studies will use a longer wavelength laser fundamental in order to reduce both resonance enhancement and absorptive losses. These will yield more accurate β_0 values and also depolarization ratios, permitting a more detailed assessment of the structural dependence of β in these new complexes.

Acknowledgements

S. H. is a Research Assistant of the Belgian National Fund for Scientific Research. This work was supported by research grants from the Royal Society, the Belgian National Fund for Scientific Research (G.2103.93 and 9.0011.92), the Belgian government (IUAP-16) and the University of Leuven (GOA/1/95). Thanks are due to Johnson Matthey plc for a generous loan of ruthenium trichloride.

References

1 S. R. Marder, in *Inorganic Materials*, eds. D. W. Bruce and D. O'Hare, Wiley, Chichester, 1992; D. R. Kanis, M. A. Ratner and T. J. Marks, *Chem. Rev.*, 1994, **94**, 195; N. J. Long, *Angew. Chem., Int. Ed. Engl.*, 1995, **34**, 21.
2 M. Schröder and T. A. Stephenson, in *Comprehensive Coordination Chemistry*, eds. G. Wilkinson, R. D. Gillard and J. A. McCleverty, Pergamon, Oxford, 1987, vol. 4.
3 W. M. Laidlaw, R. G. Denning, T. Verbiest, E. Chauchard and A. Persoons, *Nature* (*London*), 1993, **363**, 58; *Proc. SPIE, Int. Soc. Opt. Eng.*, 1994, **2143**, 14.
4 C. Dhenaut, I. Ledoux, I. D. W. Samuel, J. Zyss, M. Bourgault and H. Le Bozec, *Nature* (*London*), 1995, **374**, 339.
5 I. R. Whittall, M. G. Humphrey, A. Persoons and S. Houbrechts, *Organometallics*, 1996, **15**, 1935; S. Houbrechts, K. Clays, A. Persoons, V. Cadierno, M. P. Gamasa and J. Gimeno, *Organometallics*, 1996, **15**, 5266.
6 I. D. Morrison, R. G. Denning, W. M. Laidlaw and M. A. Stammers, *Rev. Sci. Instrum.*, 1996, **67**, 1445.
7 M. A. Mortazavi, A. Knoesen, S. T. Kowel, R. A. Henry, J. M. Hoover and G. A. Lindsay, *Appl. Phys. B*, 1991, **53**, 287.
8 D. R. Yankelevich, A. Dienes, A. Knoesen, R. W. Schoenlein and C. V. Shank, *IEEE J. Quantum Electron.*, 1992, **28**, 2398.
9 S. M. Silence, J. C. Scott, F. Hache, E. J. Ginsburg, P. J. Jenkner, R. D. Miller, R. J. Twieg and W. E. Moerner, *J. Opt. Soc. Am. B: Opt. Phys.*, 1993, **10**, 2306.
10 C. R. Moylan, *J. Phys. Chem.*, 1994, **98**, 13513.
11 K. Clays and A. Persoons, *Rev. Sci. Instrum.*, 1992, **63**, 3285.
12 E. Hendrickx, K. Clays, A. Persoons, C. Dehu and J. L. Brédas, *J. Am. Chem. Soc.*, 1995, **117**, 3547.
13 J. P. Chang, E. Y. Fung and J. C. Curtis, *Inorg. Chem.*, 1986, **25**, 4233.
14 J. C. Curtis, B. P. Sullivan and T. J. Meyer, *Inorg. Chem.*, 1983, **22**, 224.
15 S. Houbrechts, K. Clays, A. Persoons, Z. Pikramenou and J.-M. Lehn, *Chem. Phys. Lett.*, 1996, **258**, 485.
16 M. Stähelin, D. M. Burland and J. E. Rice, *Chem. Phys. Lett.*, 1992, **191**, 245.
17 S. H. Kang, Y.-M. Jeon, K. Kim, S. Houbrechts, E. Hendrickx and A. Persoons, *J. Chem. Soc., Chem. Commun.*, 1995, 635.
18 S. Maiorana, A. Papagni, E. Licandro, A. Persoons, K. Clays and S. Houbrechts, *Gazz. Chim. Ital.*, 1995, **125**, 377.
19 S. Stadler, G. Bourhill and C. Bräuchle, *J. Phys. Chem.*, 1996, **100**, 6927.
20 M. A. Pauley, H.-W. Guan, C. H. Wang and A. K.-Y. Jen, *J. Chem. Phys.*, 1996, **104**, 7821.
21 E. Hendrickx, C. Dehu, K. Clays, J. L. Brédas and A. Persoons, *ACS Symp. Ser.*, 1995, **601**, 82.
22 M. C. Flipse, R. de Jonge, R. H. Woudenberg, A. W. Marsman, C. A. van Walree and L. W. Jenneskens, *Chem. Phys. Lett.*, 1995, **245**, 297.
23 K. Clays, A. Persoons and L. De Maeyer, *Adv. Chem. Phys.*, 1994, **85**, 455.
24 S. J. Cyvin, J. E. Rauch and J. C. Decius, *J. Chem. Phys.*, 1965, **43**, 4083.
25 R. E. Clarke and P. C. Ford, *Inorg. Chem.*, 1970, **9**, 227.
26 R. E. Clarke and P. C. Ford, *Inorg. Chem.*, 1970, **9**, 495.
27 G. Jones II, W. R. Jackson, C. Choi and W. R. Bergmark, *J. Phys. Chem.*, 1985, **89**, 294.
28 A. N. Fletcher, D. E. Bliss and J. M. Kauffman, *Opt. Commun.*, 1983, **47**, 57.
29 G. A. Reynolds and K. H. Drexhage, *Opt. Commun.*, 1975, **13**, 222.
30 P. Ford, De F. P. Rudd, R. Gaunder and H. Taube, *J. Am. Chem. Soc.*, 1968, **90**, 1187.
31 M. S. Paley and J. M. Harris, *J. Org. Chem.*, 1991, **56**, 568.
32 *CRC Handbook of Chemistry and Physics*, ed. D. R. Lide, CRC Press, Boca Raton, FL, 75th edn., 1994.
33 V. Gutmann, *The Donor-acceptor Approach to Molecular Interactions*, Plenum, New York, 1978.
34 O. F. J. Noordman and N. F. Van Hulst, *Chem. Phys. Lett.*, 1996, **253**, 145.
35 J. L. Oudar and D. S. Chemla, *J. Chem. Phys.*, 1977, **66**, 2664; J. L. Oudar, *J. Chem. Phys.*, 1977, **67**, 446; J. Zyss and J. L. Oudar, *Phys. Rev. A*, 1982, **26**, 2016.

Received 18*th November* 1996; *Paper* 6/07799D